CrossMark

ORIGINAL PAPER

Lead removal from battery wastewater using synthesized poly(ethyleneglycol dimethacrylate-methacrylic acid) gel bead and poly(methacrylic acid) hydrogel

Ilda Vergili[1] · Z. Beril Gönder[1] · Yasemin Kaya[1] ·
Gülten Gürdağ[2] · Selva Çavuş[2]

Abstract This study presents the synthesis and characterization of two new polymers with the aim of Pb^{2+} ion removal from the wastewater of a battery factory. Poly(ethyleneglycol dimethacrylate-methacrylic acid) (poly(EGDMA-MAA)) gel bead and polymetacrylic acid (polyMAA) hydrogel were prepared and characterized by Fourier transform infrared spectroscopy (FTIR), thermogravimetric analysis (TGA), environmental scanning electron microscopy (ESEM), swelling capacity analysis and zeta potential measurements. Both polymers showed greater negative zeta potential values in the range of pH 3–8. Poly(EGDMA-MAA) had a relatively lower swelling capacity of 0.9 $g_{water}/g_{polymer}$ than polyMAA because of the crosslinking degree. The FTIR spectrum of the virgin poly(EGDMA-MAA) showed that the polymer has carboxylic groups to sorb the Pb^{2+} ions. The FTIR spectrum of poly(EGDMA-MAA) after sorption showed that interactions between the Pb^{2+} ions and carboxyl groups caused a decrease in the intensity of the C=O peak. The sorption experiments carried out under different conditions yielded optimal conditions of contact time and polymer amount. The Pb^{2+} adsorption capacities were found to be 1.995 and 2.047 mg g^{-1} for poly(EGDMA-MAA) and polyMAA, respectively. Moreover, the sorption mechanism was studied using kinetic and thermodynamic models. The higher R^2 (0.9997 and 0.9999), lower $\varepsilon\%$ (1.3 and 0.8) and closer values of q_{exp} and q_{cal} show that the data fit well with the type (I) pseudo-second-order model. The higher positive $\Delta S°$ value indicated that greater structural changes occurred in polyMAA than in poly(EGDMA-MAA).

✉ Ilda Vergili
  ilda@istanbul.edu.tr

1 Department of Environmental Engineering, Faculty of Engineering, Istanbul University,
   Avcilar, 34320 Istanbul, Turkey

2 Department of Chemical Engineering, Faculty of Engineering, Istanbul University, Avcilar,
   34320 Istanbul, Turkey

🖄 Springer

Introduction

Heavy metals such as lead, mercury, cadmium, nickel, zinc, and copper are typically found in industrial wastewaters at varying concentrations. The negative environmental effects of heavy metals have been known for many years. The battery industry is important with respect to the environment owing to its high consumption of water and high content of heavy metals especially lead. Preparation of reactive materials and electrolytes, deposition of reactive materials on supporting electrode structures, charging of electrodes and removing of impurities, and washing of finished cells, production equipment and manufacturing areas are the processes where water used in battery manufacturing industry. Wastewater is generated from many processes like plate curing, product rinsing, cooling, equipment and floor area washing, etc., [1]. The removal of lead ions from wastewaters plays an important role in solving the problems of industrial wastes. Lead causes several types of acute and chronic problems such as toxicity and nervous system damages in humans, especially in children [2]. The permissible lead level of water is 0.01 mg L^{-1} [3, 4]. The permissible limit for lead in wastewater is given as 3 mg L^{-1} by the Water Pollution Control Regulation in Turkey [5]. The most commonly used methods for the removal of lead ions are adsorption, precipitation, coagulation, ion exchange, electrodialysis, electrolysis, electrocoagulation and nanofiltration [6–14]. The advantages of the ion exchange method over other methods are high selectivity, the recovery of metal ions, low amount of slurry formation and achievement of the limit values. There have been several studies on the removal of lead ions from wastewaters by commercial synthetic ion exchangers [10, 15]. There have also been studies on the sorption of lead by biosorbents obtained from different materials such as banana stems [16], alginate beads [17], avocado kernel seeds [18], carrageenan [19], and hazelnut and almond shells [20]. Polymer gels are finding important applications in the removal process of heavy metal ions owing to their functional groups. Hydrogels [21, 22] and microbeads [23–25] are efficiently used toward this aim. Whereas the free radical polymerization method is employed to prepare hydrogels [21, 22], suspension polymerization is preferred for the bead form of the gels [23, 25]. In general, the ion exchange process is a common treatment process for the treatment of battery wastewater. Commercial ion exchangers are expensive and, therefore, research on low cost materials has gained importance [26]. This study aimed to investigate the use of newly synthesized gel bead and hydrogel with –COOH group for lead removal from the wastewater of a battery factory and compare the efficiency of these polymers. Based on a literature review, there is no publication about lead removal using these novel gel bead and hydrogel.

Materials and methods

Materials

Methacrylic acid (MAA), 2 ammonium peroxodisulfate (APS), N,N'-methylenebisacrylamide (NMBA), N,N,N',N'-tetramethylethylenediamine (TEMED), ethyleneglycol dimethacrylate (EGDMA) and benzoyl peroxide (BPO) were purchased from Merck Schuchardt OHG (Germany). Ultrapure water was used for all preparations. Polyvinylpyrrolidone (PVP) was obtained from ABCR GmbH & Co.KG (Karlsruhe).

Preparation of hydrogel (PolyMAA) and gel bead (Poly(EGDMA-MAA))

The hydrogel containing carboxylic acid group was synthesized in deionized water by free radical polymerization using methacrylic acid (MAA) monomer. The synthesis of hydrogels was carried out in glass tubes (with a 15 cm length and 1.3 cm inner diameter) under inert atmosphere (nitrogen) at 60 °C for 24 h. Ammonium peroxodisulfate (APS) solution, N,N'-methylenebisacrylamide (NMBA) and N,N,N',N'-tetramethylethylenediamine (TEMED) were used as initiator, cross-linking agent and accelerator, respectively. The initial monomer concentration was 1 mol L^{-1}. APS and NMBA were used as 1 and 3 mol% of the initial monomer concentration, respectively. TEMED amount was equal to that of initiator in weight. Obtained hydrogels were sliced into pieces and placed into deionized water up to unreacted contents are removed. After then, drying process was applied first in air and then in vacuum oven at 40 °C.

Gel beads containing carboxylic acid group were synthesized by suspension polymerization method from MAA and ethyleneglycol dimethacrylate (EGDMA) in the presence of benzoyl peroxide (BPO) and polyvinylpyrrolidone (PVP) as initiator and stabilizer, respectively. TEMED was used as the accelerator in the synthesis of gel beads. While the MAA (4 mL), EGDMA (8 mL) and BPO (0.4 g) take place in organic phase, to prepare dispersion medium, a known amount of polyvinylpyrrolidone (PVP) was dissolved within 50 mL of deionized water. Total reaction volume is 100 mL. The preparation of gels (poly(EGDMA-MAA)) was performed in a glass polymerization reactor with a constant stirring rate of 500 rpm at 70 °C under nitrogen atmosphere. After preparation and cleaning, gel beads were first dried in air, and then in vacuum oven at constant temperature (40 °C).

Wastewater

The wastewater used in the experiments was obtained from a battery manufacturing company in Istanbul, Turkey. The characteristics of the battery wastewater are given in Table 1. The concentrations of the other metal ions present in the wastewater were very low that they could not affect the removal of lead ions by ion exchange.

Table 1 The characteristics of the battery wastewater

Characteristics	Value
pH	2.0
Conductivity	7.83 mS cm^{-1}
Pb	4.46 mg L^{-1}
Mn	0.1 mg L^{-1}
Ni	0.097 mg L^{-1}
Cu	0.083 mg L^{-1}
Cr	0.070 mg L^{-1}
Zn	0.029 mg L^{-1}
Ag	0.002 mg L^{-1}
As	3.3 μg L^{-1}
Cd	3.2 μg L^{-1}
Sn	13.9 μg L^{-1}

Instrumentation and characterization

In all cases, the samples were analyzed using a Perkin Elmer flame and graphite-furnace atomic absorption spectrometers (AAS). The AAS provides a detection limit of 0.01 mg L^{-1} for lead. The measurements were repeated three times, and the average values were taken as the remaining metal amount in the solution phase. The maximum deviation was 1.0%.

The ESEM images were used to determine the interactions between the polymers and the Pb^{2+} ions. The samples of the polymers were fractured using liquid nitrogen and were subsequently coated with gold to obtain an adequate contrast of the polymer structure. The ESEM images were obtained using a JEOL/JSM- 6335F-INCA instrument with an accelerating voltage of 10.0 kV.

FTIR (Perkin-Elmer Spectrum One FTIR Spectrometer) was used to identify the difference between the synthesized polymers (gel bead or hydrogel) before and after sorption. The FTIR data were obtained using the KBr pellet method, and the FTIR spectra were recorded in the wavenumber range of 600–4000 cm^{-1}.

TGA for the polymers and the Pb^{2+} ion sorbed at equilibrium by the polymer was carried out within a temperature range from 30 °C to 800 °C at a rate of 20 °C min^{-1} under a nitrogen atmosphere (flowrate of 20 mL min^{-1}) using a Shimadzu DTG 60 instrument. All samples were in dried form.

The zeta potentials of the polymer particles in deionized water were measured using a Particle Size Analyzer (Brookhaven Instruments BIC 90 Plus) according to the method of Alkan et al. [27]. The measurements were taken at different pH values (2–9). The pH of the samples was monitored using a pH meter (Thermo Orion 3-Star model).

In the determination of the equilibrium swelling values of the gel bead and hydrogel, a known weight of the dry polymer was immersed in deionized water at room temperature and held there until swelling equilibrium was reached, and then its swollen form was weighed. The following equation was used to determine the equilibrium swelling values of polymers.

$$\text{Equilibrium swelling value:} \left(g_{\text{water}} / g_{\text{polymer}} \right) = \left(W_{\text{s}} - W_{\text{d}} \right) / W_{\text{d}} \qquad (1)$$

where W_{s} and W_{d} are the weights of swollen and dry polymers, respectively.

Lead removal studies

The removal of Pb^{2+} from the battery wastewater by hydrogel (polyMAA) and gel bead (poly(EGDMA-MAA)) polymers was investigated using batch experiments. All experimental tests were carried out in duplicate and the average values were used for further calculations.

The batch experiments were carried out at $25 \pm 2\ °C$ in a thermostated orbital shaker at an agitation speed of 200 rpm. Aliquots of the wastewater (50 mL) were added to a given amount of the polymers in stoppered glass Erlenmeyer flasks. The pH of the wastewater was maintained at 5.0 using $0.1\ \text{mol L}^{-1}$ NaOH. pH value of 5 is preferred in the experiments since lead is predominated as positively charged Pb^{2+} ions at this pH [10]. Blanks with distilled water were also used to assess the losses of solutes to the flask components during the batch tests. The results of the duplicate tests showed that the average solution phase concentrations were within 98–102% of the respective initial concentration of the same solution analyzed in a similar manner. Hence, the loss of solute was negligible. The supernatants were filtered through 0.45 μm Whatman filter papers to determine the Pb^{2+} concentration using AAS.

The amounts of sorbed Pb^{2+} ion at equilibrium by the polymer were calculated using the formula

$$q_{\text{e}} = (C_0 - C_{\text{e}}) \frac{V}{W} \qquad (2)$$

where q_{e} is the amount of Pb^{2+} ion sorbed at equilibrium (mg g^{-1}), C_0 is the initial Pb^{2+} ion concentration, C_{e} is the equilibrium concentration of Pb^{2+} ions in solution (mg L^{-1}), V is the volume of the wastewater (L), and W is the weight of the polymer (g) [28].

The applicability of the kinetic models to describe the ion exchange process, apart from the correlation coefficient (R^2), was further validated by the average percentage errors ($\varepsilon\%$) between the experimental and predicted values calculated using the formula as defined by Aksu and Kabasakal [29].

Results and discussion

Polymer characterization studies

The zeta potential measurements

The zeta potentials were measured to observe the surface charge of hydrogel (polyMAA) and gel beads (poly(EGDMA-MAA)) at different pH values (Fig. 1). At pH 2, the zeta potential value is positive for both polymers. At this pH, the ion
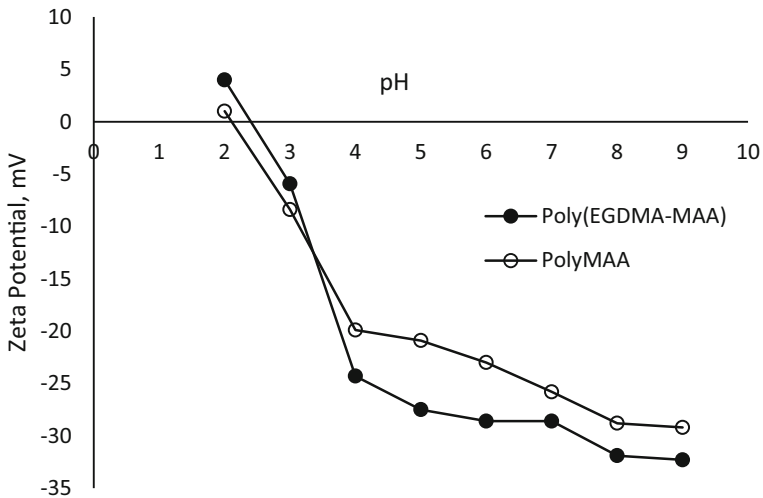
Fig. 1 Zeta potentials of gel bead and hydrogel as a function of pH

exchange of Pb^{2+} was not expected. For gel beads (poly(EGDMA-MAA)), the increase in pH from 3 to 8 resulted in decreased zeta potentials from -5.9 to -32 mV. Moreover, the increase in pH led to a decrease in the zeta potentials of hydrogel (polyMAA) up to -30 mV. The negative zeta potentials may be attributed to the dissociation of carboxylic (–COOH) and, to a less extent, phenolic (–OH) groups at these pH values [30].

Swelling capacity

The swelling is related to chain mobility and crosslinking degree. The swelling capacity decreases with increased crosslinking. Higher swelling capacity means a higher quantity of water in the polymer molecular chains [31]. The equilibrium swelling value of the gel bead and hydrogel were found to be 0.9 and 21 $g_{water}/g_{polymer}$, respectively. Hydrogel has a higher swelling capacity, whereas the relatively lower swelling capacity of the gel beads could be attributed to the crosslinking degree.

ESEM images

The ESEM images of hydrogel (polyMAA) and gel beads (poly(EGDMA-MAA)) before and after sorption at different temperatures are shown in Figs. 2 and 3, respectively. As clearly seen in Fig. 2a, the gel beads have a spherical form. The virgin gel bead has a near-smooth surface (Fig. 2b). After sorption, the ESEM images of gel beads display much rougher and more irregular surface structures with increasing temperatures. The gel beads are strongly crosslinked polymers compared with hydrogels. Although they do not dissolve in wastewater, lower swelling value of the gel bead is remarkable. As seen in Fig. 2c, e, g, the good condition of the
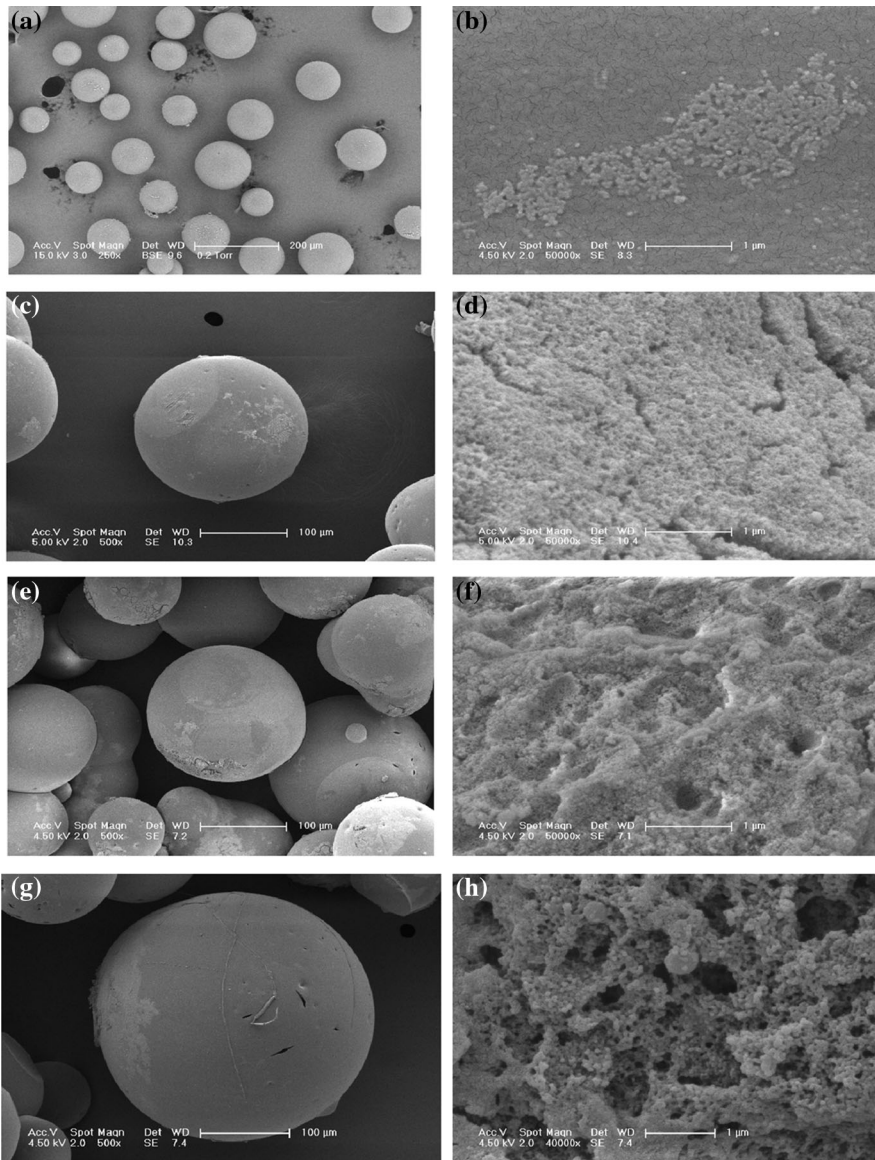
Fig. 2 ESEM images of the poly(EGDMA-MAA) *before* and *after* sorption at different temperatures: **a** virgin gel bead, **b** virgin gel bead, **c** 298 K, **d** 298 K, **e** 308 K, **f** 308 K, **g** 318 K, **h** 318 K

spherical morphology is evidence of the stability of gel beads. The beads are quite rigid. Wrinkled surfaces of gel beads after sorption may be attributed to the shrinkage of the beads at high temperatures (Fig. 2d, f, h). As an example ESEM images of hydrogels before and after sorption at different temperatures are depicted in Fig. 3. The surface morphology of the hydrogel is totally different from the gel
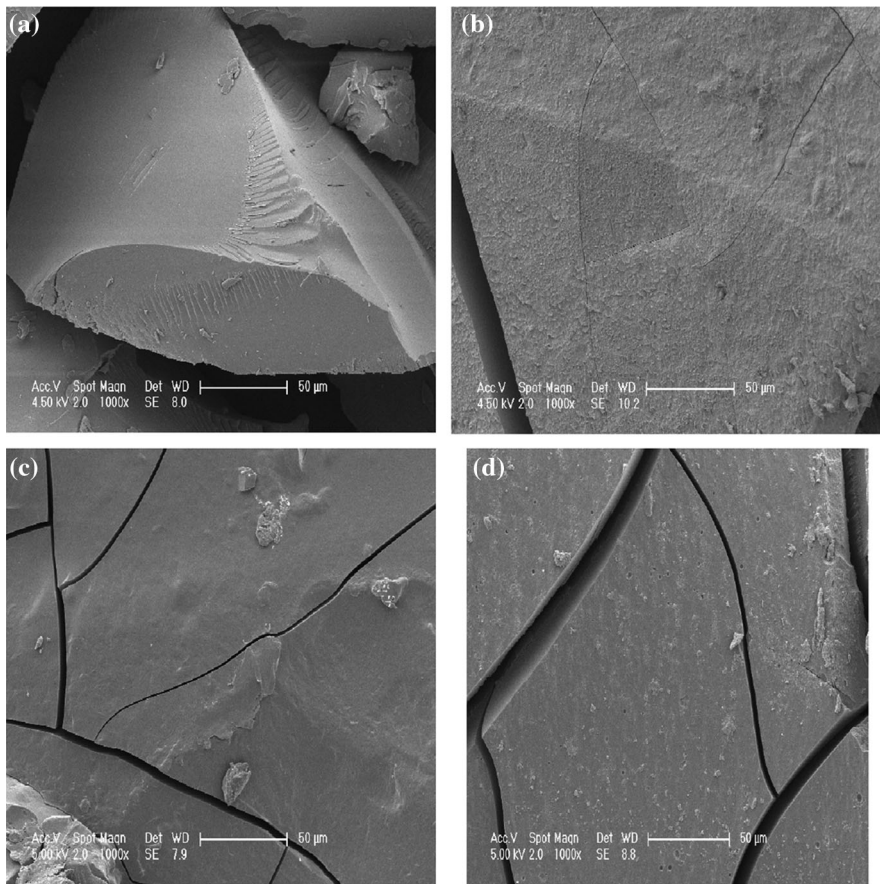
Fig. 3 ESEM images of polyMAA *before* and *after* sorption: **a** virgin hydrogel, **b** 298 K, **c** 308 K, **d** 318 K

bead as expected. Hydrogel has a smooth but cracked surface. After sorption, the surface is less rough with respect to the gel beads.

FTIR spectra

The surface functional groups of hydrogel (polyMAA) and gel bead (poly(EGDMA-MAA)) before and after sorption (298 K) were characterized using FTIR spectra (Fig. 4). The FTIR spectrum for the virgin gel bead polymer shows a band of absorbance between 3000 and 3600 cm^{-1} (centered at 3565 cm^{-1}), which is attributed to the O–H stretching of the surface carboxylic groups [32]. The bands at 2989 and 2958 cm^{-1} are due to the stretching vibration of the C–H bond [33]. Additionally, the band at 1729 cm^{-1} is due to the C=O stretching of the carboxyl groups [32] and indicates the C=O stretching band of the ester functionality of EGDMA [34]. The band at 1637 cm^{-1} may be associated with the carbonyl groups of carboxylic acid [35]. The band at 1455 cm^{-1} corresponds to the asymmetric CH$_3$
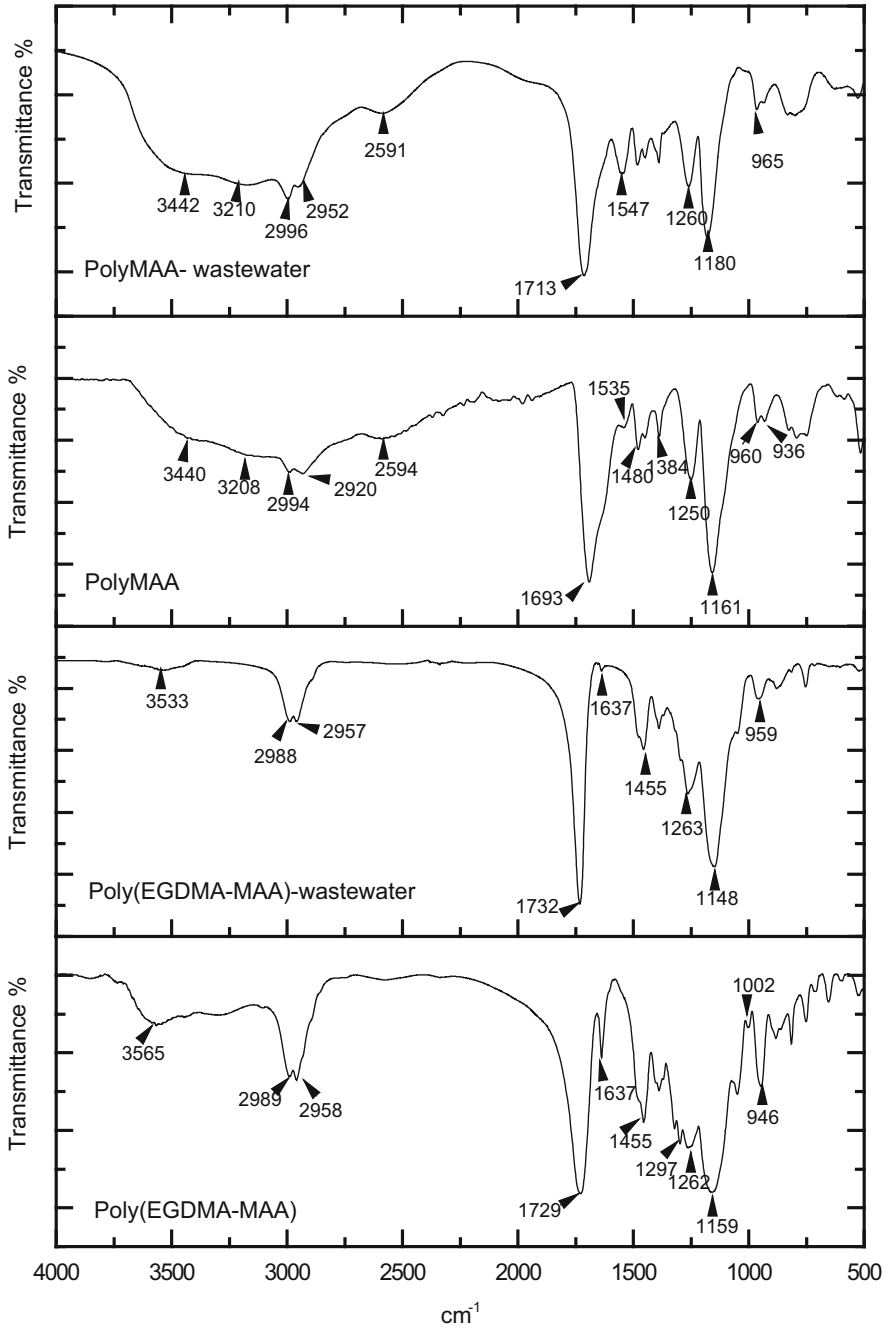
Fig. 4 FTIR spectra of hydrogel (polyMAA) and gel bead (poly(EGDMA-MAA)) *before* and *after* sorption

bending band [36]. The peak at 1159 cm^{-1} represents C–O–C bending. The FTIR spectrum of the virgin gel bead confirms that the gel bead has the carboxylic groups to sorb the Pb^{2+} ions. Furthermore, the bands are consistent with a commercial weak acidic polymer with a carboxylic group [10]. The most evident change in the spectrum of gel bead after sorption is the shift and diminishment of the 3533 cm^{-1} band. This could be attributed to the sorption of Pb^{2+} ions via ion exchange between the –COOH groups and the Pb^{2+} ions. This result is most likely due to the weakening of the inter- and intramolecular hydrogen bonds in the ion exchange of Pb^{2+} [36]. The band at 1732 cm^{-1} is not altered, whereas the signal at 1637 cm^{-1} is strongly reduced. Two bands at 1297 and 1262 cm^{-1} in the spectrum of virgin gel bead are available as a single band at 1263 cm^{-1} after sorption. The band at 1159 cm^{-1} is shifted to 1148 cm^{-1}, and the intensity of the band is decreased. Furthermore, the band at 946 cm^{-1} is shifted to a higher wavelength (959 cm^{-1}), and a loss in intensity is observed. As a result, it can be said that interaction between the Pb^{2+} ions and carboxyl groups caused the decrease in the intensity of the C=O peak [37].

In the aforementioned region, absorption bands are clearly observed at 3440, 3208, 2994, 2920, 2594, 1693, 1535, 1480, 1384, 1250, 1161, 960 and 936 cm^{-1} for polyMAA. After sorption, no new absorption bands are observed. The positions of the bands at which their intensities change owing to Pb^{2+} ion sorption via ion exchange between –COOH groups and Pb^{2+} ions are at 1693, 1535, 1250, and 1161 cm^{-1}. The band at 1693 cm^{-1} is shifted to a higher wavelength (1713 cm^{-1}), and a loss in intensity is observed. An evident change in the spectrum of the hydrogel was the shift of the 1535 cm^{-1} band to 1547 cm^{-1}. Moreover, the intensity of the band is increased. Furthermore, the band at 1161 cm^{-1} is shifted to a higher wavelength (1180 cm^{-1}), and a loss in intensity is observed.

Thermal characterization

TGA was used to investigate the thermal properties and Pb^{2+} sorbed forms of polymers. The TGA curves are represented and compared in Fig. 5. It is evident that the degradation steps and curve profiles for the gel beads and hydrogel are different. In addition, TGA revealed that polymers were more thermally stable after sorption. The hydrogel was thermally decomposed in a greater number of steps compared with that of the gel bead counterparts. However, the main backbone decomposition step in the gel beads was larger. After the sorption process, polyMAA displayed higher thermal stability than virgin polyMAA. A similar situation was not observed for the gel beads. The thermal behavior of poly(EGDMA-MAA) samples before and after sorption were approximately the same. This could be attributed to the rigid nature of gel beads owing to the higher amount of cross-linker. The mass loss ratio at different temperatures was determined from the corresponding TGA thermograms. For poly(EGDMA-MAA), the mass loss was observed to be 2.2 and 1.9% before and after sorption, respectively, at 200 °C. However, 11.4 and 14% mass loss was seen at 200 °C before and after sorption for polyMAA, respectively. At 350 °C, mass losses were found to be 48.7 and 37.5% for poly(EGDMA-MAA) before and after sorption, respectively. Mass losses were 26.2 and 27.9% for polyMAA before
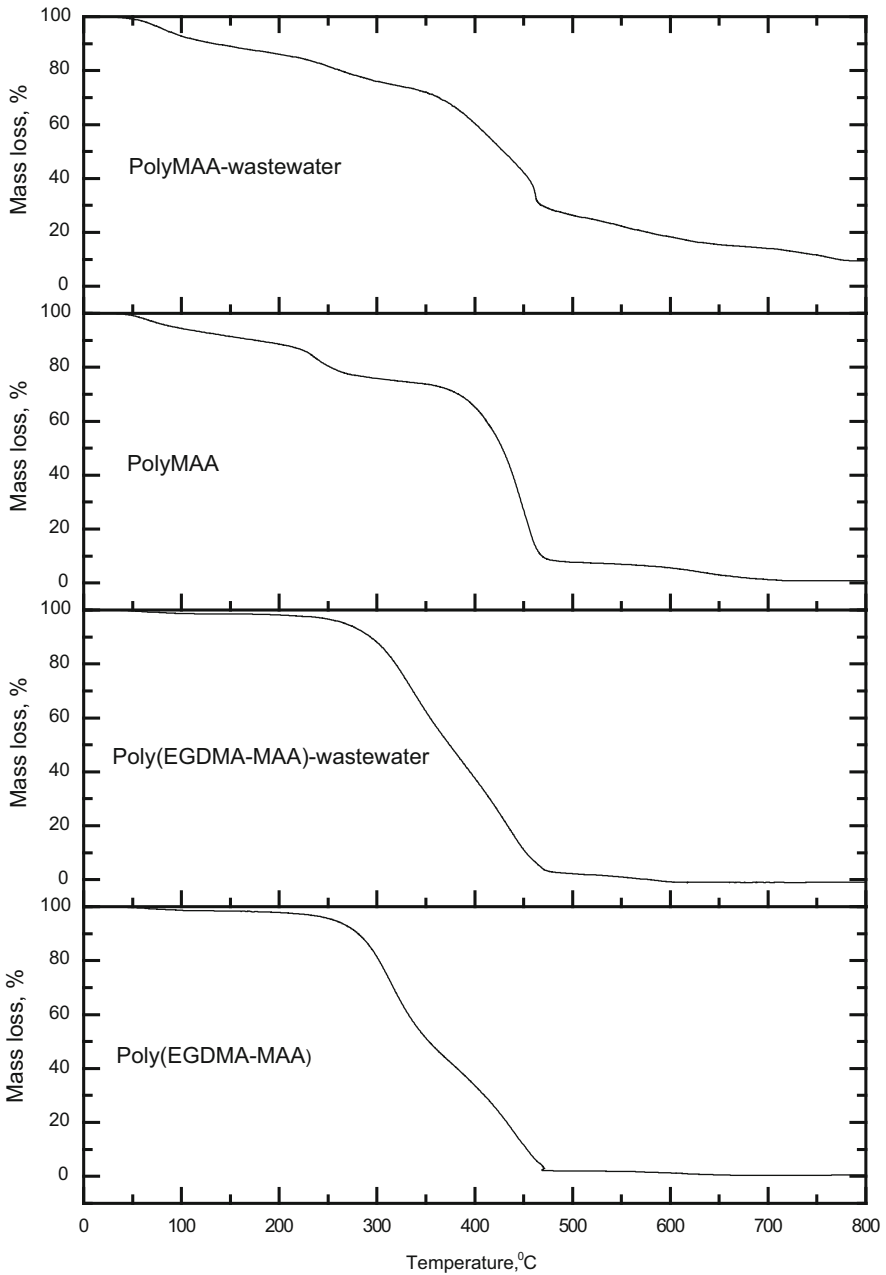
Fig. 5 TGA thermograms of hydrogel (polyMAA) and gel bead (poly(EGDMA-MAA) *before* and *after* sorption

and after sorption, respectively. The total mass loss was 88.5% at 450 °C for poly(EGDMA-MAA) before and after sorption, whereas 72.9 and 57.9% mass losses were found for polyMAA before and after sorption, respectively.

Lead removal studies

The batch studies were composed of two sections: in the first section, the effects of the amount of polymer (m), contact time (t) and temperature (T) on the sorption of Pb^{2+} onto the polymers were examined. In the second section, the sorption mechanism under various conditions was investigated using kinetic and thermo-dynamic models.

Effect of the amount of polymer

Determining the optimal amount of polymer is an important stage in determining the maximum possible Pb^{2+} removal. For this purpose, a series of wastewater samples (50 mL) were shaken at varying polymer dosages (0.01−0.2 g) at 25 ± 2 °C. The optimal amount of polymer was found to be 0.1 g (2 g L^{-1}) for hydrogel (polyMAA) and gel beads (poly(EGDMA-MAA)) with sorption capacities of 2.05 and 1.995 mg g^{-1}, respectively.

Effect of contact time

Figure 6 shows the effect of the contact time on the sorption of Pb^{2+}. As seen, removal efficiencies increased with increasing contact time for both polymers. The required equilibrium time for hydrogel (polyMAA) was found to be 90 min. Eighty-two percent of Pb^{2+} sorption was completed in the first 5 min, which increased to 91% in 90 min. Interestingly, a rapid uptake and establishment of equilibrium in a short period (30 min) was observed when using gel beads (poly(EGDMA-MAA)).
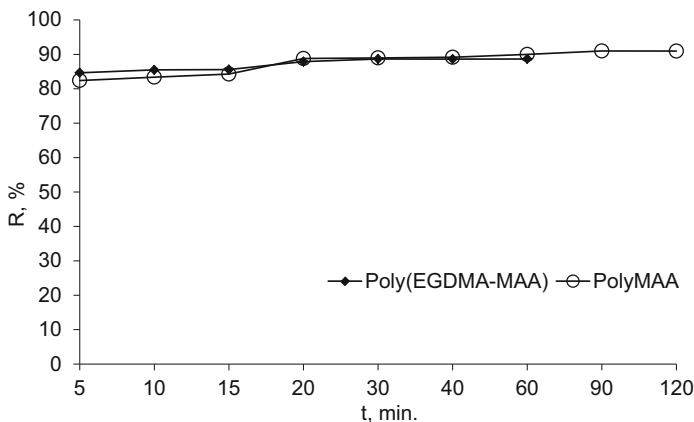

Fig. 6 Effect of contact time on the Pb^{2+} removal from battery wastewater by hydrogel (polyMAA) and gel beads (poly(EGDMA-MAA))

Eighty-five percent removal of Pb^{2+} was obtained within 5 min which increased to 89% in 30 min. Owing to such a quick sorption rate it can be inferred that physical interaction is predominant in this sorption process. The ionic functional groups in the hydrogel structure are mainly responsible for the removal of Pb^{2+} ions from wastewater [38]. However, the sorption process also occurs at the surface of the gel beads because of the complexations between sorbate and functional groups [30]. In that case, it is expectable that lead ions more easily and rapidly reach the active binding sites of the gel bead compared with hydrogel.

The sorption capacities of gel beads and hydrogel at equilibrium conditions were found to be 1.995 and 2.05 mg g^{-1}, respectively. The capacities of the synthesized gel beads and hydrogel are low in comparison to the studies that carried out with aqueous solutions [39]. However, in our previous study [10], Pb^{2+} sorption capacity of a commercial weak acid resin with –COOH functional groups was found as 4.95 mg g^{-1} for lead concentration of 5 mg L^{-1} from aqueous solution. So, it could be said that the sorption capacities of newly synthesized gel beads and hydrogel for a real wastewater are found to be satisfactory.

Effect of temperature and thermodynamics

The effect of temperature on Pb^{2+} removal was studied in the range of 298–318 K for various time intervals using hydrogel (polyMAA) and gel beads (poly(EGDMA-MAA)). The removal efficiencies increased with increasing temperature (Fig. 7). Whereas 7% difference was observed between the removal efficiencies of the experiments carried out at 298 and 318 K with PMAA hydrogel, a 9% increase in the removal efficiency of gel beads was determined with the increase in temperature in the same range. The effect of temperature was relatively low indicating that the removal mechanism is solely that of ion exchange [40].

The amounts of sorbed Pb^{2+} at equilibrium at different temperatures (298–318 K) were used to evaluate the thermodynamic parameters. The Gibbs free energy change ($\Delta G°$) and the equilibrium constant (K_c) are calculated according to Eqs. (3, 4). The plot of ln K_c as a function of $1/T$ yields a straight line from which the enthalpy change
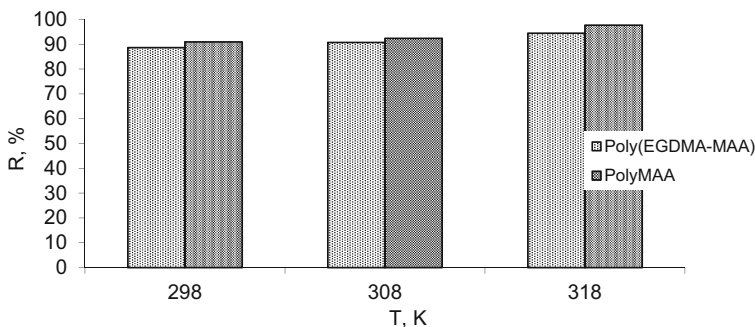

Fig. 7 Effect of temperature on Pb^{2+} removal by hydrogel (polyMAA) and gel beads (poly(EGDMA-MAA)

Table 2 Estimated thermodynamic parameters at different temperatures (298–318 K)

Thermodynamic parameters	Poly(EGDMA-MAA)			PolyMAA		
	298 K	308 K	318 K	298 K	308 K	318 K
K_c	7.8	9.8	17.2	10.1	12.2	43.1
ΔG (kJ mol^{-1})	−5096.7	−5849.0	−7513.1	−5725.5	−6396.6	−9951.3
ΔH (kJ mol^{-1})	+30,755.2			+56,758.9		
ΔS (J mol^{-1} K^{-1})	+119.8			+208.2		

($\Delta H°$) and entropy change ($\Delta S°$) are calculated from the slope and intercept of Eq. (5), respectively.

$$\Delta G° = -RT \ln K_c \tag{3}$$

$$K_c = \frac{C_{Re}}{C_{Se}} \tag{4}$$

$$\ln K_c = \frac{-\Delta H°}{RT} + \frac{\Delta S°}{R} \tag{5}$$

where R is the gas constant (8.314 J mol^{-1} K^{-1}), T is the temperature (K), C_{Re} is the equilibrium concentration of the sorbed Pb^{2+} (mg L^{-1}) and C_{Se} is the equilibrium concentration of the Pb^{2+} in the solution (mg L^{-1}) [41].

The estimated thermodynamic parameters at different temperatures (298–318 K) are shown in Table 2. The overall $\Delta G°$ values during the process at all studied temperatures were negative, corresponding to a spontaneous process of Pb^{2+} ion sorption onto both polymers. The decreased values of $\Delta G°$ with increasing temperature indicated that sorption of Pb^{2+} was more effective at higher temperature [42]. Moreover, the K_c values increased with increasing temperature owing to the increased mobility of molecules, indicating an endothermic reaction. The increase in K_c values with increasing temperature was found to be more dramatic for hydrogel (from 10.1 to 43.1). Additionally, the positive values of the enthalpy change indicated that the process was endothermic for both polymers. The positive and high $\Delta H°$ values provide evidence that a good interaction occurred between the polymers and the Pb^{2+} ions. The hydrogel polymer showed the best interaction with the highest $\Delta H°$ value of +56,758.9 kJ mol^{-1}. The $\Delta S°$ parameter indicates the affinity of the polymer. The positive values of $\Delta S°$ correspond to an increase in randomness in the ongoing process at the solid–liquid interface and may indicate that significant changes occurred in the internal structure of the polymers through the sorption of Pb^{2+} ions [42]. The highest positive $\Delta S°$ value was obtained for the hydrogel. Consequently, it can be said that the changes in the structure of the hydrogel were greater than those of the gel beads because of the rigid nature of the gel bead.

Kinetics

Reaction-based kinetic models were used to investigate the mechanism of Pb^{2+} sorption onto gel beads and hydrogel. The rate of sorption for the Pb^{2+} ions was determined using the Lagergren pseudo-first order and types 1–5 pseudo-second order. The kinetic parameters were calculated using the mathematical equations for reaction-based kinetic models as defined by Vergili et al. [10]. The Lagergren pseudo-first-order model is used when the rate of occupation of the binding sites is proportional to the number of unoccupied sites on the polymer [43]. If the pseudo-first-order kinetic does not properly account for the kinetics of the process, the pseudo-second-order kinetics may be applied. This model is applied when the rate
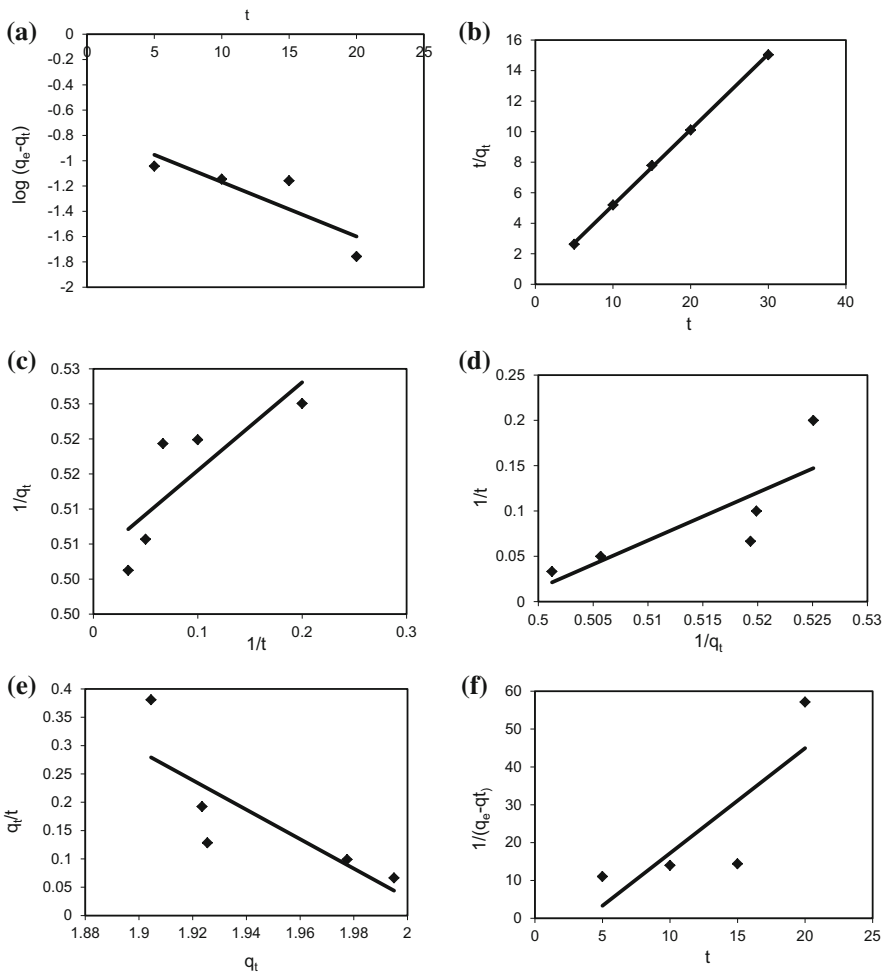

Fig. 8 Reaction kinetic models for the sorption of Pb^{2+} by poly(EGDMA-MAA): **a** pseudo-first-order, **b** type 1 pseudo-second-order, **c** type 2 pseudo-second-order, **d** type 3 pseudo-second-order, **e** type 4 pseudo-second-order, **f** type 5 pseudo-second-order

Fig. 9 Reaction kinetic models for the sorption of Pb^{2+} by polyMAA: **a** pseudo-first-order, **b** type 1 pseudo-second-order, **c** type 2 pseudo-second-order, **d** type 3 pseudo-second-order, **e** type 4 pseudo-second-order, **f** type 5 pseudo-second-order
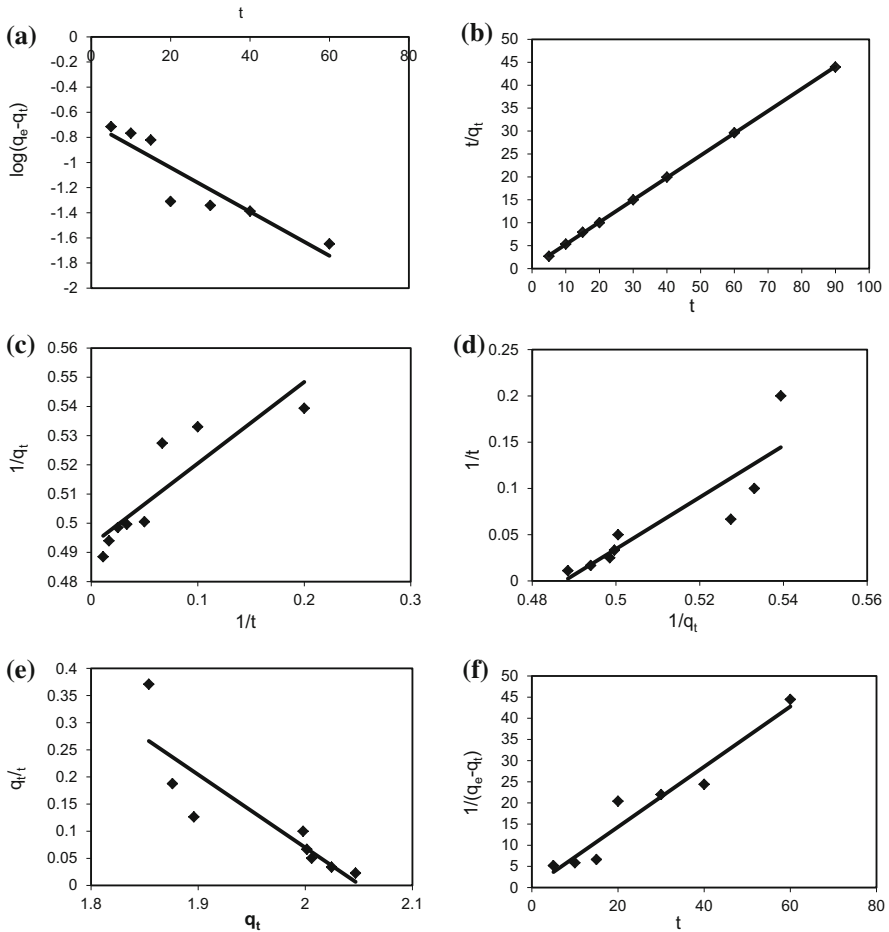
of occupation of sites is proportional to the square of the number of unoccupied sites on the polymer [44]. The second order rate constant, k_2 (g mg^{-1} min^{-1}) is used to calculate the initial sorption rate constant, h (mg g^{-1} min^{-1}) [41].

Figures 8 and 9 show the plots obtained by applying the reaction-based kinetic models to the sorption data of gel beads and hydrogel. The kinetic parameters calculated using the reaction kinetic models are listed in Table 3. The higher R^2 (0.9997 and 0.9999), lower $\varepsilon\%$ (1.3 and 0.8) and closer values of q_{exp} and q_{cal} show that the data fit well with the type (I) pseudo-second-order model. The pseudo-second-order reactions are greatly affected by the amount of metal on the polymer's surface and the amount of sorbed metal at equilibrium. The rate is directly proportional to the number of active surface sites [44]. Although the sorption capacities of gel beads and hydrogel were too close (Table 3), the Pb^{2+} sorption

Table 3 Estimated parameters for the reaction kinetic models

Reaction base kinetic models	Parameters	Poly(EGDMA-MAA)	PolyMAA
Lagergren pseudo-first-order	q_{exp} (mg g^{-1})	1.995	2.047
	q_{cal} (mg g^{-1})	0.183	0.204
	k_1 (L g^{-1})	0.099	0.040
	R^2	0.7327	0.8417
	$\varepsilon\%$	90.8	90.0
Type 1 pseudo-second-order	q_{exp} (mg g^{-1})	1.995	2.047
	q_{cal} (mg g^{-1})	2.021	2.063
	k_2 (g mg^{-1} min^{-1})	1.045	0.520
	h (mg g^{-1} min^{-1})	4.268	2.213
	R^2	0.9997	0.9999
	$\varepsilon\%$	1.3	0.8
Type 2 pseudo-second-order	q_{exp} (mg g^{-1})	1.995	2.047
	q_{cal} (mg g^{-1})	1.989	2.030
	k_2 (g mg^{-1} min^{-1})	2.012	0.870
	h (mg g^{-1} min^{-1})	7.960	3.585
	R^2	0.6652	0.7788
	$\varepsilon\%$	0.3	0.8
Type 3 pseudo-second-order	q_{exp} (mg g^{-1})	1.995	2.047
	q_{cal} (mg g^{-1})	2.011	2.051
	k_2 (g mg^{-1} min^{-1})	1.308	0.664
	h (mg g^{-1} min^{-1})	5.290	2.793
	R^2	0.6652	0.7788
	$\varepsilon\%$	0.8	0.2
Type 4 pseudo-second-order	q_{exp} (mg g^{-1})	1.995	2.047
	q_{cal} (mg g^{-1})	2.012	2.052
	k_2 (g mg^{-1} min^{-1})	1.292	0.655
	h (mg g^{-1} min^{-1})	5.230	2.758
	R^2	0.6539	0.7683
	$\varepsilon\%$	0.9	0.2
Type 5 pseudo-second-order	q_{exp} (mg g^{-1})	1.995	2.047
	q_{cal} (mg g^{-1})	-0.095	7.987
	k_2 (g mg^{-1} min^{-1})	2.7736	0.7111
	h (mg g^{-1} min^{-1})	0.025	45.356
	R^2	0.6592	0.9345
	$\varepsilon\%$	–	–

mechanisms of the studied polymers are different from each other. The pseudo-second-order rate constant (k_2) value of the Pb^{2+} sorption onto gel beads was two-fold greater than the k_2 value of the Pb^{2+} sorption onto hydrogel. Moreover, the initial sorption rate (h) value of Pb^{2+} onto gel beads was 1.9 times greater than that of Pb^{2+} ion onto hydrogel. The sorption of Pb^{2+} onto gel bead was faster during the

initial sorption process. The faster initial rate of Pb^{2+} ion sorption for gel bead could be attributed to the large number of available sorption sites and more accessible surface for the Pb^{2+} leading to faster removal by gel beads. Moreover, the driving force effect of mass transfer should be considered because both the surface properties of the polymers and their physical shapes are quite different, which affects the sorption mechanism. Increased initial sorption rate values of the gel bead could be attributed to the increase in the driving force for mass transfer. Shorter times were needed to reach the surface of the sorbents owing to the increase in the driving force for mass transfer [45].

Conclusions

This study investigated the synthesis of polymers containing –COOH groups with the aim of Pb^{2+} removal from the wastewater of a battery factory. A comparison of the two different types of polymers was performed and successful results were obtained in terms of polymer synthesis and application. Gel beads (poly(EGDMA-MAA)) and hydrogel (PolyMAA) could be considered to have a remarkable removal ability of low Pb^{2+} concentrations in wastewater from the battery industry with removal rates of 89% and 91%, respectively. The sorption capacities of gel beads and hydrogel were found to be 1.995 and 2.05 mg g^{-1}, respectively. Although the sorption capacities were similar, the Pb^{2+} sorption mechanisms were found to be different. It can be concluded that Pb^{2+} ions more easily and rapidly reach the active binding sites of gel beads compared with hydrogel. The twofold greater pseudo-second-order rate constant (k_2) value and the initial sorption rate (h) value of the gel beads supported this result. Neither the rigid structure of the gel beads nor the less rigid (more swellable) structure of the hydrogel were affected. The FTIR spectra of both polymers proved that the polymers have carboxylic groups to sorb the Pb^{2+} ions.

References

1. EPA (1984) Battery manufacturing effluent guidelines. https://www.epa.gov/eg/battery-manufacturing-effluent-guidelines. Accessed 22 Nov 2016
2. Manahan SE (1999) Environmental chemistry. Lewis, Boca Raton
3. TS266 (2005) Turkish standards for water intended for human consumption
4. WHO (2011) World Health Organization, lead in drinking water, background document for development of WHO guidelines for drinking water quality
5. WPCR (2004) Water pollution control regulation, Republic of Turkey Ministry of Environment and Urban
6. Taty-Costodes VC, Fauduet H, Porte C, Hoh YS (2005) Removal of lead (II) ions from synthetic and real effluents using immobilized pinus sylvestris sawdust: adsorption on fixed-bed column. J Hazard Mater B123:135–144
7. Macchi G, Pagano M, Santori M, Tiravanti G (1993) Battery industry wastewater: Pb removal and produced sludge. Water Res 27:1511–1518

8. Pang FM, Kumar P, Teng TT, Omar AKM, Wasewar KL (2011) Removal of lead, zinc and iron by coagulation. J Taiwan Inst Chem Eng 42:809–815

9. Pagano M, Petruzzelli D, Tiravanti G, Passino R (2000) Pb/Fe separation and recovery from automobile battery wastewaters by selective ion exchange. Solvent Extr Ion Exc 18:387–399

10. Vergili I, Soltobaeva G, Kaya Y, Gönder ZB, Çavuş S, Gürdağ G (2013) Study of the removal of Pb(II) using a weak acidic cation (WAC) polymer: kinetics, thermodynamics, equilibrium and breakthrough curves. Ind Eng Chem Res 52:9227–9238

11. Gherasim C-V, Křivčík J, Mikulášek P (2014) Investigation of batch electrodialysis process for removal of lead ions from aqueous solutions. Chem Eng J 256:324–334

12. Abou-Shady A, Peng C, Bi J, Xu H, Almeria OJ (2012) Recovery of Pb(II) and removal of NO3− from aqueous solutions using integrated electrodialysis, electrolysis, and adsorption process. Desalination 286:304–315

13. Mansoorian HJ, Mahvi AH, Jafari AJ (2014) Removal of lead and zinc from battery industry wastewater using electrocoagulation process: Influence of direct and alternating current by using iron and stainless steel rod electrodes. Sep Purif Technol 135:165–175

14. Mehdipour S, Vatanpour V, Kariminia H-Z (2015) Influence of ion interaction on lead removal by a polyamide nanofiltration membrane. Desalination 362:84–92

15. Qian J, Zeng Z, Xue W, Guo Q (2015) Lead removal from aqueous solutions by 732 cation-exchange resin. Can J Chem Eng 94:142–150

16. Noeline BF, Manohar DM, Anirudhan TS (2005) Kinetic and equilibrium modelling of lead (II) sorption from water and wastewater by polymerized banana stem in a batch reactor. Sep Purif Technol 45:131–140

17. Salisu A, Sanagi MM, Abu Naim A, Abd Karim KJ, Ibrahim WAW, Abdulganiyu U (2016) Alginate graft polyacrylonitrile beads for the removal of lead from aqueous solutions. Polym Bull 73:519–537

18. Diaz-Munoz LL, Bonilla-Petriciolet A, Reynel-Avila HE, Mendoza-Castillo DI (2016) Sorption of heavy metal ions from aqueous solution using acid-trated avocado kernel seeds and its FTIR spectroscopy characterization. J Mol Liq 215:555–564

19. Giri TK, Verma D, Tripathi DK (2015) Effect of adsorption parameters on biosorption of Pb^{++} ions from aqueous solution by poly (acrylamide)-grafted kappa-carrageenan. Polym Bull 72:1625–1646

20. Pehlivan E, Altun T, Cetin S, Bhanger MI (2009) Lead sorption by waste biomass of hazelnut and almond shell. J Hazard Mater 167:1203–1208

21. Rodríguez E, Katime I (2003) Behavior of acrylic acid-itaconic acid hydrogels in swelling, shrinking, and uptakes of some metal ions from aqueous solution. J Appl Poym Sci 90:530–536

22. Atta AM, Ismail HS, Elsaaed AM (2012) Application of anionic acrylamide-based hydrogels in the removal of heavy metals from wastewater. J Appl Poym Sci 123:2500–2510

23. Duran A, Soylak M, Tuncel SA (2008) Poly(vinyl pyridine-poly ethylene glycol methacrylate-ethylene glycol dimethacrylate) beads for heavy metal removal. J Hazard Mater 155:114–120

24. Iemma F, Cirillo G, Spizzirri UG, Puoci F, Parisi OI, Picci N (2008) Removal of metal ions from aqueous solution by chelating polymeric microspheres bearing phytic acid derivatives. Eur Polym J 44:1183–1190

25. Kara A, Demirbel E (2012) Kinetic, isotherm and thermodynamic analysis on adsorption of Cr(VI) ions from aqueous solutions by synthesis and characterization of magnetic-poly (divinylbenzene-vinylimidazole) microbeads. Water Air Soil Poll 223:2387–2403

26. Kannan N, Seenivasan RK (2006) Synthesis, characterization, and application of new low-cost ion exchangers. J Appl Polym Sci 101:4104–4113

27. Alkan M, Karadas M, Dogan M, Demirbas Ö (2005) Adsorption of CTAB onto perlite samples from aqueous solutions. J Colloid Interf Sci 291:309–318

28. Vergili I, Barlas H (2009) Removal of 2,4-D, MCPA and metalaxyl from water using lewatit VP OC 1163 as sorbent. Desalination 249:1107–1114

29. Aksu Z, Kabasakal E (2004) Batch adsorption of 2,4-dichloropheoxy-acetic acid (2,4-D) from aqueous solution by granular activated carbon. Sep Purif Technol 35:223–240

30. Yan WL, Bai R (2005) Adsorption of lead and humic acid on chitosan hydrogel beads. Water Res 39:688–698

31. Leitão RCF, de Moura CP, da Silva LD, Ricardo MPS, Feitosa JPA, Muniz EC, Fajardod AR, Rodriguesa FHA (2015) Novel superabsorbent hydrogel composite based on poly(acrylamide-co-acrylate)/nontronite: characterization and swelling performance. Quím Nova 38:370–377

32. Yoon IH, Meng X, Wang C, Kim KW, Bang S, Choe E, Lippincott L (2009) Perchlorate adsorption and desorption on activated carbon and anion exchange resin. J Hazard Mater 164:87–94

33. Stuart B (2004) Infrared spectroscopy: fundamentals and applications. Wiley, West Sussex
34. Huang C-W, Sun Y-M, Huang W-F (1997) Curing kinetics of synthesis of poly(2-hydroxyethyl metacrylate) (PHEMA) with ethylene glycol dimethacrylate (EDGMA) as a crosslinking agent. J Polym Sci A Polym Chem 35:1873–1889
35. Poacco G, Cascone MG, Petarca L, Peretti A (2000) Thermal behaviour of poly(methacrylic acid)/poly(N-vinyl-2-pyrrolidone) complexes. Eur Polym J 36:2541–2544
36. Cavus S, Gurdag G, Sozgen K, Gurkaynak MA (2009) The preparation and characterization of poly(acrylic acid-co-methacrylamide) gel and its use in the non-competitive heavy metal removal. Polym Adv Technol 20:165–172
37. Marambio OG, Pizarro GD, Jeria-Orell M, Huerta M, Olea-Azar C, Habicher WD (2005) Poly(N-phenylmaleimide-co-acrylic acid)-copper(II) and poly(N-phenylmaleimide-co-acrylic acid)-cobalt(II) complexes: synthesis, characterization, and thermal behavior. J Polym Sci Pol Chem 43:4933–4941
38. Milosavljević NB, Ristić MD, Perić-Grujić AA, Filipović JM, Štrbac SB, Rakočević ZL, Krušić MTK (2010) Hydrogel based on chitosan, itaconic acid and methacrylic acid as adsorbent of Cd^{2+} ions from aqueous solution. Chem Eng J 165:554–562
39. Yang L, Li Y, Jin X, Ye Z, Ma X, Wang L, Liu Y (2011) Synthesis and characterization of a series of chelating resins containing amino/imino-carboxyl groups and their adsorption behavior for lead in aqueous phase. Chem Eng J 168:115–124
40. Muraviev D, Gonzalo A, Valiente M (2000) Ion Exchange on resins with temperature-responsive selectivity III. Influence of complex formation stoichiometry on temperature dependence of resin selectivity. J Chromatogr A 868:143–152
41. Dizge N, Keskinler B, Barlas H (2009) Sorption of Ni (II) ions from aqueous solution by lewatit cation-exchange resin. J Hazard Mater 167:915–926
42. Islam M, Patel R (2009) Removal of lead (II) from aqueous environment by a fibrous ion exchanger: polycinnamamide thorium (IV) phosphate. J Hazard Mater 172:707–715
43. Kumar D, Gaur JP (2011) Chemical reaction-and particle diffusion-based kinetic modeling of metal biosorption by a phormidium sp.-dominated cyanobacterial mat. Bioresour Technol 102:633–640
44. Ho YS, McKay G (1999) The sorption of lead (II) ions on peat. Water Res 33:578–584
45. Sulak MT, Demirbas E, Kobya M (2007) Removal of astrazon yellow 7GL from aqueous solutions by adsorption onto wheat bran. Bioresour Technol 98:2590–2598